

Influence of anode and cathode plasmas on the operation of an electronic diode with an explosive-emission cathode

© A.I. Pushkarev, S.S. Polisadov

Tomsk Polytechnic University,
634050 Tomsk, Russia
e-mail: aipush@mail.ru

Received August 11, 2021

Revised November 9, 2021

Accepted November 10, 2021

The results of modeling and experimental investigation of the formation of anode and cathode plasmas in a vacuum diode with an explosive-emission cathode during the generation of a pulsed electron beam with a current density of $0.3\text{--}0.4 \text{ kA/cm}^2$ and an accelerating voltage of $300\text{--}500 \text{ kV}$ are presented. It is shown that the concentration of the anode plasma does not exceed 10^{10} cm^{-3} and it does not significantly contribute to the operation of the diode. However, the complete desorption of molecules from the working surface of the explosive-emission cathode and the high efficiency of shock ionization of atoms ensure the formation of a cathode gas plasma with a concentration of $\approx 10^{16} \text{ cm}^{-3}$. It is found that the charge of the explosive-emission plasma layer is significantly less than the charge of the electron beam and the main source of electrons is not an explosive-emission plasma, but a cathode gas plasma. In this case, the electron current is limited by the concentration of the cathode plasma. The use of a cathode with a developed surface (a cathode with a carbon fabric coating) allows increasing the total charge of the electron beam by more than 1.5 times without changing the cathode diameter and the anode-cathode gap.

Keywords: high-current electron beam, explosive emission, plasma concentration, electronically stimulated desorption.

DOI: 10.21883/TP.2022.02.52946.234-21

Introduction

Vacuum diodes with an explosive-emission cathode are widely used to generate pulsed electron beams [1]. Many researchers note a considerable contribution of adsorbed gas to diode operation. The monograph by G.A. Mesyats [2] showed that residual gas pressure and the method of obtaining vacuum in a chamber affects the stability of the current from the cathode. Upon a transition from oil-free high vacuum to oil pumping-out and pressure rise to 0.1 Pa , cathode operation stability is higher, their lifetime is more than 10^6 pulses. Monograph [3] and papers [4,5] present the results of study of a metal-ceramic cathode made of oxide nanoceramics, across the bulk of which metal particles are uniformly distributed. The authors suppose that cathode plasma is generated due to the development of a discharge in gas in near-surface micropores between the dielectric and the metal. A significant contribution of gas liberation to operation of explosive-emission cathodes with a felt and velvet coating during generation of electron beams with a current density of $20\text{--}30 \text{ A/cm}^2$ and with an accelerating voltage of $300\text{--}400 \text{ kV}$ is noted in [2].

Generation of an electron beam with a high current density is accompanied with electron-stimulated desorption of gas from the anode, formation of anode plasma and its propagation into the anode-cathode (AC) gap [2]. Anode plasma is one of the essential factors restricting the duration of an electron beam pulse produced by a diode with an

explosive-emission cathode [6]. Total diode current in such conditions can exceed the quantity determined by the one-dimensional Child–Langmuir (CL) equation [7] due to reduction of the AC-gap, due to additional compensation of the bulk charge of electrons in the near-cathode region by ions from anode plasma and other factors. The relationship of these processes affecting the operation of a vacuum diode with an explosive-emission cathode has been poorly studied. Article [8] presents an analysis of the current-voltage characteristic of a planar diode with a graphite cathode 5 cm in diameter when a voltage pulse is applied (300 kV , 100 ns). It has been demonstrated that when the initial AC-gap is 6 mm , total diode current is satisfactorily described by a CL with account of AC-gap reduction by cathode plasma which expands at a constant rate ($2.5\pm0.1 \text{ cm}/\mu\text{s}$). When the initial AC-gap decreased to 2.8 mm , total current 50 ns after voltage application exceeded the calculated values, which, in the authors opinion, is due to the compensation of the bulk charge by anode plasma ions.

Our paper [9] presents the results of study of the impact of adsorbed gas on the operation of a diode with an explosive-emission cathode during generation of a high-current electron beam ($300\text{--}500 \text{ kV}$, 80 ns). The impact was determined according to a change in cathode plasma expansion rate. It was found that plasma rate in case of different AC-gaps is constant during the beam generation, but is different for cathodes made of different materials. It was $2\pm0.5 \text{ cm}/\mu\text{s}$ for graphite and carbon fiber cathodes

of a different diameter, $3 \pm 0.5 \text{ cm}/\mu\text{s}$ for a multi-needle tungsten cathode, $3.5 \pm 0.5 \text{ cm}/\mu\text{s}$ for a copper solid and a copper multi-point cathode. The considerable dependence of plasma rate on cathode material shows that the impact of adsorbed gas on operation of a diode with an explosive-emission cathode is insignificant.

An essential condition for efficient generation of an electron beam in a diode with a passive cathode is plasma formation on the cathode working surface. Plasma in a diode with an explosive-emission cathode formed during explosive emission of electrons, which forms a heterogeneous structure of plasma. Separate emissive centers originate at the first stage [2], the minimum distance between them is determined by the effect of electric field shielding around the center [10]. Shielding radius is 5–6 mm in case of electron current from one emissive center equal to 90 A [11] and an accelerating voltage during generation of emissive centers equal to 100–120 kV. The average plasma concentration in an emissive center within 5 to 20 ns after voltage application drops from 10^{17} to $5 \cdot 10^{15} \text{ cm}^{-3}$ [12]. It was demonstrated in [13] that cathode plasma concentration in a diode with a carbon fibre cathode is $5 \cdot 10^{15} \text{ cm}^{-3}$. It was demonstrated in [14] that concentration of the explosive-emission plasma in the cathode region is 10^{14} cm^{-3} , and then it drops back in proportion to squared distance. The distribution of concentration of explosive-emission plasma of a graphite cathode is described by relation $(9 \cdot 10^{14})/x^2, \text{cm}^{-3}$ with x in millimeters [15]. A continuous plasma layer forms due to expansion of separate emissive centers, therefore cathode plasma concentration can restrict electron current density. The performed studies were aimed at analyzing the impact of anode and cathode plasma on the operation of a vacuum diode with an explosive-emission cathode upon generation of a high-current electron beam.

1. Experimental setup

The studies have been carried out on the TEU-500 pulsed accelerator (300–500 kV, 80 ns) [16]. Fig. 1 shows the diode assembly of the accelerator and diagnostic equipment.

We used a diode with a flat cylindrical cathode 60 mm in diameter, made of different materials, AC-gap was 12 mm. The anode was the flat copper collector of the Faraday cup 92 mm in diameter. Fig. 2 shows the oscilloscope traces of accelerating voltage and electron current. Accelerating voltage was measured by a capacitance divider placed in an oil-filled chamber and by a differential voltage divider placed in the vacuum space of the diode chamber [17]. Total current of the electron beam was measured using a Faraday cup which was evacuated together with the diode chamber to a pressure of 5–10 mPa.

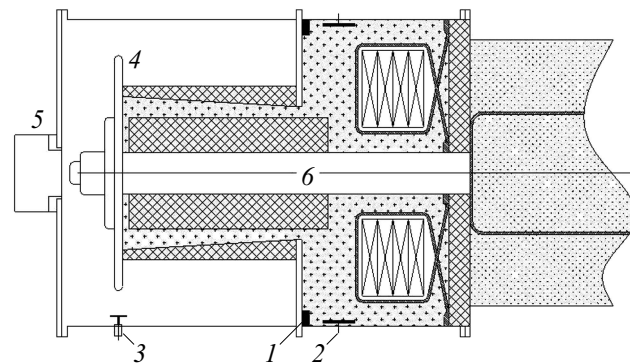


Figure 1. Diagnostic equipment of the TEU-500 pulsed electron accelerator: 1 — Rogowski coil, 2 — capacitance divider, 3 — differential voltage divider, 4 — potential disk of the diode, 5 — Faraday cup, 6 — cathode holder.

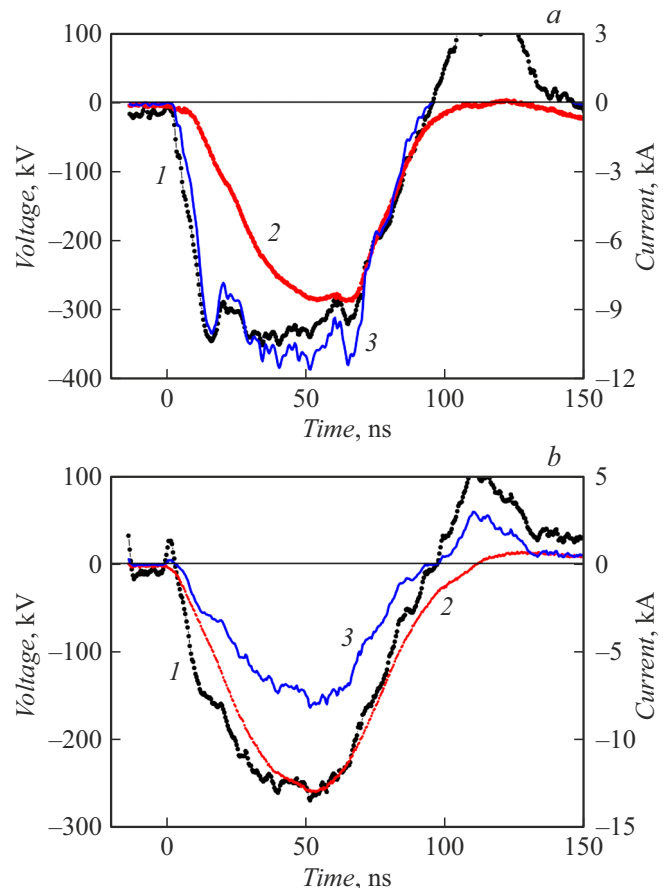


Figure 2. Oscilloscope traces of accelerating voltage (1) and electron current (2). Curve 3 shows the calculated current. Cathode made of graphite (a) and with carbon fiber coating (b).

Fig. 2 also shows the calculated values of diode current. The calculation was performed using the relation [18]:

$$I_e(t) = \frac{4\epsilon_0\sqrt{2e}}{9\sqrt{m_e}} \cdot \frac{S_{cath} \cdot U^{3/2}}{d(t)^2} \\ = 2.33 \cdot 10^{-6} \cdot U^{3/2} \cdot \frac{\pi(r_0 + v_{expl} \cdot t)^2}{(d_{AC} - v_{expl} \cdot t)^2}, \quad (1)$$

where S_{cath} — cathode area, U — accelerating voltage, ϵ_0 — absolute permittivity, r_0 — cathode radius, d_{AC} — initial AC-gap, m_e — electron mass, e — electron charge, v_{expl} — expansion rate of explosive-emission plasma.

2. Calculation of anode plasma concentration

Anode plasma in a vacuum diode is generated upon exposure of the anode working surface to an electron beam, electron-stimulated desorption of molecules, their dissociation and ionization of atoms near the anode. Electron-stimulated desorption provides the molecules with additional kinetic energy, since it is caused by excitation of the atom electron subsystem [19] and this energy is not wholly consumed during spent desorption. As shown in [20], the kinetic energy spectrum of molecules during electron-stimulated desorption of methanol from an aluminum surface has a maximum at an energy of 0.1–0.2 eV and speed distribution of molecules considerably differs from the Boltzmann distribution. It was demonstrated in [21,22] that the energy spectrum of N₂O molecules after electron-stimulated desorption from the Ru surface reaches a maximum at an energy of 0.13–0.15 eV. In our experiments, the composition of the residual gas in the diode chamber and the adsorbed molecules corresponds to the composition of the air. When the energy of nitrogen and oxygen molecules after desorption is 0.15 eV, the anode gas layer will expand at the rate of 0.17 cm/μs and its thickness during electron beam generation will be less than 0.14 mm. Therefore, electron energy in the anode gas layer exceeds 100 keV at an accelerating voltage of 300–500 kV.

Calculation of anode plasma concentration along the cross-section of shock ionization is hindered due to the absence of reliable values of the ionization cross-section at an electron energy of over 5 keV [23]. Anode plasma concentration in the AC-gap can be calculated on the basis of linear losses of electron energy (LLE), since at an energy below 1 MeV the main contribution to energy losses upon absorption in a target is made by ionization processes [24].

Let the concentration of molecules in the anode gas layer be constant throughout the volume and decrease during electron current generation due to gas layer expansion at a constant rate. Then the average anode plasma concentration is equal to

$$n_{an}(t) = \frac{N_{sum}(t)}{V_{gas}(t)} = \frac{N_{sum}(t)}{S_{an} \cdot v_{gas1} \cdot t} [\text{cm}^{-3}], \quad (2)$$

where $N_{sum}(t)$ — total number of ions generated in the anode gas layer, $V_{gas}(t)$ — volume of the anode gas layer, S_{an} — anode working area, $v_{gas1} = \text{const}$ — expansion rate of the anode gas layer.

The total number of ions, generated in the anode gas layer during electron beam generation, is equal to a double integral of the product of the number of ions, generated by one electron on unit path $N(E)$, and the number of electrons

generated per unit time, with integration by duration of the electron current pulse and by the AC-gap:

$$N_{sum}(t) = \int_0^{d_{AC}} \int_0^{\tau} N(E) \frac{I_e(t)}{e} dx dt, [\text{ions}], \quad (3)$$

where $I_e(t)$ is electron current in the diode, [A], τ is pulse duration.

Number of ions generated on a unit path in the AC-gap by one electron of energy E is equal to

$$N(E) = \frac{1}{E_{sum}} \frac{dE}{dx}, [\text{ions/cm}], \quad (4)$$

where dE/dx is LLE, [eV/cm], E_{sum} is the sum of energy of molecular dissociation and atom shock ionization, [eV].

In our experiments, composition of residual gas in the diode chamber and adsorbed molecules matches the air composition, therefore in the calculations we adopted $E_{sum} = 23$ eV taking into account dissociation of N₂ and O₂ molecules, ionization of nitrogen and oxygen atoms and their partial pressure in air.

LLE were calculated using the ESTAR program [25] as per the NIST data. Fig. 3 shows the dependence of LLE in the air at 1 atm and 300 K.

Dependence of LLE on electron energy for subsequent calculations was approximated by the function

$$\begin{aligned} \frac{dE}{dx} &= 48.9 - 36.7[1 - \exp(0.11E)] \\ &- 9.9[1 - \exp(0.016E)], [\text{keV/cm}], \end{aligned} \quad (5)$$

where E is electron energy, [keV].

LLE were calculated in the ESTAR program for molecule concentration $n_0 = 2.7 \cdot 10^{19} \text{ cm}^{-3}$. Molecular dissociation and shock ionization of atoms take place due to binary shocks of the electron (with a molecule or atom), therefore LLE are proportional to molecule concentration. Then, the number of ions generated by one electron of energy E on a unit path in the gas layer with molecule concentration $n_{gas1}(t)$ is equal to:

$$N(E) = \frac{n_{gas1}(t)}{n_0 \cdot E_{sum}} \frac{dE}{dx}, [\text{ions/cm}]. \quad (6)$$

LLE at an electron energy above 100 keV do not exceed 5 keV/cm and vary insignificantly (Fig. 3), therefore the change in electron energy and magnitude of LLE in the anode gas layer and during beam generation in relation (3) can be neglected:

$$\begin{aligned} N_{sum}(t) &= \int_0^{d_{AC}} \int_0^{\tau} N(E) \frac{I_e(t)}{e} dx dt \\ &= \frac{n_{gas1}(t) \cdot d_{AC}}{n_0 \cdot e \cdot E_{sum}} \frac{dE}{dx} \int_0^{\tau} I_e(t) dt, [\text{ions}]. \end{aligned} \quad (7)$$

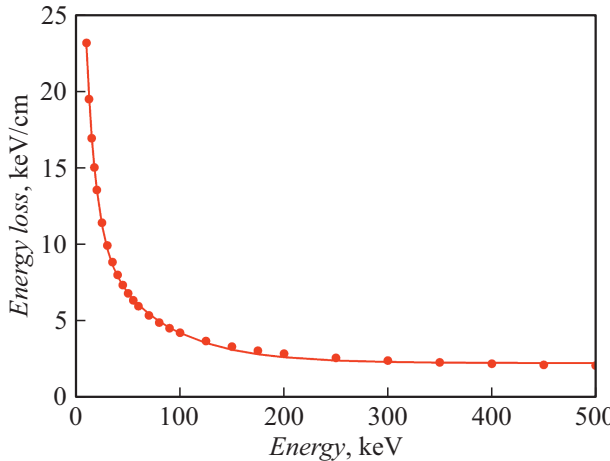


Figure 3. Dependence of linear losses of electron energy on its energy [25].

When the molecule concentration in the anode gas layer is 10^{13} – 10^{14} cm $^{-3}$, the molecule concentration in the remaining volume of the AC-gap is $\sim 10^{12}$ cm $^{-3}$. Therefore, anode plasma mainly forms in the anode gas layer of thickness d_{an} and in ratio (7) $d_{AC} \approx d_{an}$ and $n_{gas1} \cdot d_{an} = n_{s0} - n_s(t)$, where $n_s(t)$ is surface density of adsorbed molecules on the anode, [cm $^{-2}$], n_{s0} is the initial surface density of adsorbed molecules. Then the total number of ions, which are formed in the anode gas layer during electron beam generation, is equal to

$$N_{sum}(t) = \frac{[n_{s0} - n_s(t)]}{n_0 \cdot e \cdot E_{sum}} \frac{dE}{dx} \int_0^\tau I_e(t) dt, [\text{ions}]. \quad (8)$$

Rate of decrease of surface density of adsorbed molecules on the anode during electron beam generation is equal to [26, 27]:

$$\frac{dn_s(t)}{dt} = -\sigma_{des} \cdot \phi_e(t) \cdot n_s(t), [\text{cm}^{-2} \cdot \text{s}^{-1}], \quad (9)$$

where σ_{des} is cross-section of electron-stimulated desorption of molecules, [cm 2]; $\phi_e(t)$ is electron flux density on the anode surface, [cm $^{-2} \cdot \text{s}^{-1}$].

Let the electron current density be constant along the beam cross-section. The average (for the anode working area) electron flux density is equal to

$$\phi_e(t) = \frac{I_e(t)}{S_{an} \cdot e}, [\text{cm}^{-2} \cdot \text{s}^{-1}]. \quad (10)$$

Then rate of decrease of surface density of adsorbed molecules on the anode during electron beam generation is equal to

$$\frac{dn_s(t)}{dt} = -\frac{\sigma_{des} \cdot I_e(t) \cdot n_s(t)}{S_{an} \cdot e}, [\text{cm}^{-2} \cdot \text{s}^{-1}]. \quad (11)$$

Cross-section of electron-stimulated desorption of molecules is within 10^{-22} cm 2 [28,29] to 10^{-16} cm 2 [30,31].

Cross-section of electron-stimulated desorption of oxygen molecules from a titanium target at the temperature of 300 K is 10^{-19} – 10^{-18} cm 2 [32]. Experimental data on cross-section of electron-stimulated desorption of nitrogen molecules from a copper target are not available. It was demonstrated in [19] that cross-section of electron-stimulated desorption does not greatly depend on electron energy. When the cross-section of electron-stimulated desorption is below 10^{-18} cm 2 and the initial surface density of adsorbed molecules on the anode is 10^{16} cm $^{-2}$, their surface density during electron beam generation (80 ns, Fig. 2) will decrease by less than 10^{12} cm $^{-2}$. This change in surface density of adsorbed molecules on the anode can be neglected and relation (11) can be written as

$$\frac{dn_s(t)}{dt} = -\frac{n_{s0} \cdot \sigma_{des}}{S_{an} \cdot e} I_e(t), [\text{cm}^{-2} \cdot \text{s}^{-1}]. \quad (12)$$

Then surface density of adsorbed molecules on the anode will decrease during electron beam generation following the relation

$$n_s(t) = n_{s0} - \frac{\sigma_{des} \cdot n_{s0}}{S_{an} \cdot e} \int_0^\tau I_e(t) dt, [\text{cm}^{-2}]. \quad (13)$$

The following is obtained from relations (2), (8) and (13)

$$n_{an}(t) = \frac{\sigma_{des} \cdot n_{s0}}{S_{an}^2 \cdot t \cdot v_{gas1} \cdot e^2 \cdot n_0 \cdot E_{sum}} \frac{dE}{dx} \times \left[\int_0^\tau I_e(t) dt \right]^2, [\text{cm}^{-3}]. \quad (14)$$

Relation (14) takes into account a change in molecule concentration in the anode gas layer due to an increased number of desorbed molecules and gas layer expansion during electron beam generation. This relation also takes into account a change in the number of electrons in case of a change in electron current and LLE change due to changing accelerating voltage.

In our experimental conditions, the angle of electron dispersal in the AC-gap is 130 ± 5 degrees [16] and in case of the cathode diameter of 6 cm, AC-gap of 1.2 cm, anode area exposed to an electron beam is equal to 75 cm^2 . In our calculations it is assumed that nitrogen and oxygen molecules after desorption have the energy of 0.15 eV and the anode gas layer expands at the rate of 0.17 cm/ μ s. Then the average anode plasma concentration for the electron-stimulated desorption cross-section of 10^{-18} cm 2 is equal to

$$n_{an}(t) = \frac{6.6 \cdot 10^5}{t} \frac{dE}{dx} \left[\int_0^\tau I_e(t) dt \right]^2, [\text{cm}^{-3}] \quad (15)$$

where current is in kA, time is in ns, dE/dx is in keV/cm.

The calculation results using relation (15) are shown in Fig. 4.

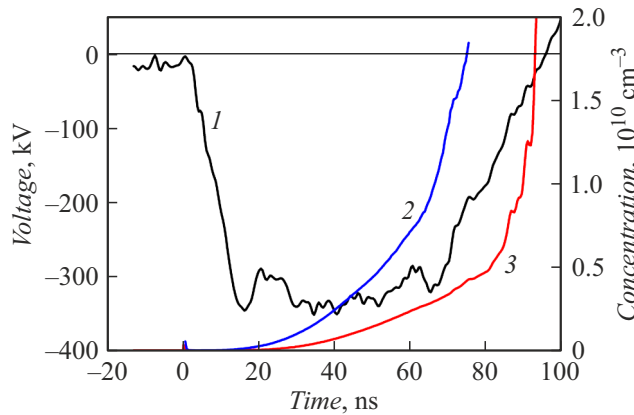


Figure 4. Oscilloscope trace of accelerating voltage (1) and a change in anode plasma concentration during electron beam generation. Cathode made of graphite (2) and with carbon fiber coating (3).

Fig. 4 also shows the results of the calculation of a change in anode plasma concentration during electron beam generation by a diode with a carbon fiber-coated aluminum cathode (Fig. 2, b).

The anode plasma concentration was calculated on condition that the surface density of molecules on the anode does not decrease in a series of pulses. Density of the molecule flow to the anode is equal to

$$\phi_a = \frac{n_0 \cdot v_m}{4} = \frac{n_0}{4} \sqrt{\frac{3k_B T}{m_a}}, \text{ [cm}^{-2}\text{s}^{-1}\text]},$$

where m_a is molecule mass, v_m is its average speed, k_B is the Boltzmann constant.

Concentration of residual gas molecules in the diode chamber at the pressure of 10 mPa is $2.7 \cdot 10^{12} \text{ cm}^{-3}$. The average speed of oxygen and nitrogen molecules at the temperature of 300 K is equal to $(4.8-5.2) \cdot 10^4 \text{ cm/s}$. Then density of molecule flow to the anode will be $(1.3-1.4) \cdot 10^{17} \text{ cm}^{-2}\text{s}^{-1}$.

Paper [33] presents the results of study of molecule desorption from the target surface by laser radiation ($\lambda = 1.06 \mu\text{m}$) in a vacuum chamber at the pressure of $2 \cdot 10^{-9} \text{ Pa}$. The studies were carried out with lead, copper and titanium targets at the temperature of 300 K, the exposure region area was 0.03 cm^2 . It was established that the number of desorbed molecules is equal to $5 \cdot 10^{14}$, which corresponds to their surface density before irradiation $\approx 2 \cdot 10^{16} \text{ cm}^{-2}$. When density of the molecule flow to the anode is $\approx 10^{17} \text{ cm}^{-2}\text{s}^{-1}$, monolayer formation duration will be less than 0.1 s. Pulse-repetition rate in our experiments does not exceed 2 pulses per second, and the equilibrium surface density of adsorbed molecules on the diode electrodes recovers between the pulses.

In our experimental conditions, one electron desorbs maximum one molecule from the anode surface ($\sigma_{des} n_{s0} < 1$). It was shown in [6] that the impact of a

pulsed electron beam with the electron energy of 10 keV on the anode surface leads to desorption of gas molecules, efficiency being 1–2 molecules per electron.

Recombination of anode plasma is possible in the course of electron beam generation. Anode plasma ionization degree is $\sim 10^{-3}$, therefore, recombination takes place at three-particle interaction of an electron, ion and atom, recombination rate is equal to [34,35]:

$$\frac{dn_e}{dt} = -\beta \cdot n_i \cdot n_e \cdot n_{gas1} \approx -\beta \cdot n_{an}^2 \cdot n_{gas1}, \text{ [cm}^{-3}\text{s}^{-1}\text]}, \quad (16)$$

where β is the recombination rate constant.

The recombination rate constant is equal to [36]

$$\beta = 5.4 \cdot 10^{-27} \cdot Z^3 \cdot T_e^{-4.5}, \text{ [cm}^6/\text{s}],$$

where T_e is electron temperature of anode plasma in eV, Z is ionization multiplicity.

The recombination rate constant for singly-ionized ions and $T_e = 1 \text{ eV}$ is equal to $5.4 \cdot 10^{-27} \text{ cm}^6/\text{s}$.

The recombination rate constant can be also calculated using relation [34,37]:

$$\beta = \frac{10^{-14} \sigma_0}{I} \left(\frac{I}{T_e} \right)^{4.5}, \text{ [cm}^6/\text{s}],$$

where $\sigma_0 \approx 10^{-16} \text{ cm}^2$ is gas-kinetic cross-section, I is ionization energy.

The recombination rate constant at the ionization energy of 14 eV and anode plasma electron temperature of 1 eV is equal to $1 \cdot 10^{-26} \text{ cm}^6/\text{s}$. The anode plasma recombination rate at the recombination rate constant of $(0.54-1.0) \cdot 10^{-26} \text{ cm}^6/\text{s}$ is equal to $(4-7) \cdot 10^{-12} \text{ cm}^{-3} \cdot \text{s}^{-1}$ and anode plasma concentration will decrease by 10^{-50} % within 80 ns. Therefore, recombination makes an insignificant contribution to anode plasma concentration change during electron beam generation.

The anode plasma concentration was calculated for the electron-stimulated desorption cross-section of 10^{-18} cm^2 , which is the maximum value of oxygen molecule desorption from a titanium target [32]. Therefore, average anode plasma concentration in a diode with a graphite cathode by the pulse end does not exceed 10^{10} cm^{-3} , anode plasma region thickness is 0.014 cm, molecule concentration in the anode gas layer is $\approx 10^{13} \text{ cm}^{-3}$, while anode plasma ionization degree is less than 10^{-3} . An increase of electron current in a diode with a carbon fiber-coated cathode causes an increase in anode plasma concentration.

3. Calculation of cathode plasma concentration

An anode gas layer of nitrogen and oxygen molecules expands with the rate of $\sim 0.17 \text{ cm}/\mu\text{s}$ and in 80 ns its thickness will be 0.014 cm. Expansion rate of explosive-emission plasma is equal to $2-4 \text{ cm}/\mu\text{s}$ [13], therefore, the

AC-gap will be mainly filled with explosive-emission plasma. However, a layer of adsorbed molecules was located on the cathode surface prior to explosive emission. At the leading edge of the accelerating voltage pulse, all these molecules are desorbed and move in the form of an expanding gas layer on the front of explosive-emission plasma. During the pulse, electrons are accelerated in the AC-gap from the emission boundary of explosive-emission plasma, dissociate molecules and ionize atoms in the gas layer on the plasma front. Electron energy in this case is below $e \cdot U$ and LLE in the cathode gas layer considerably increase (Fig. 3).

3.1. Calculation according to linear losses of energy

Let the concentration of molecules in the cathode gas layer is constant throughout the volume and decrease during its expansion with a constant rate, and let the electron current density is constant along the cross-section and vary during beam generation. Then the average cathode plasma concentration is equal to

$$n_{cath1} = \frac{N_{sum2}(t)}{S_{cath} \cdot v_{gas2} \cdot t}, \text{ [cm}^{-3}\text]}, \quad (17)$$

where $N_{sum2}(t)$ is the total number of ions forming in the cathode gas layer at shock ionization; S_{cath} is cathode working area; $v_{gas2} = \text{const}$ is expansion rate of the cathode gas layer.

$N_{sum2}(t)$ was calculated similarly to relation (3):

$$N_{sum2}(t) = \int_0^{d_{AC}} \int_0^{\tau} N_2(E) \frac{I_e(t)}{e} dx dt, \text{ [ions].} \quad (18)$$

The number of ions generated by one electron of energy E on a unit path in the cathode gas layer with molecule concentration $n_{gas2}(t)$ is equal to

$$N_2(E) = \frac{n_{gas2}(t)}{n_0 \cdot E_{sum}} \frac{dE}{dx}(x, t), \text{ [ions/cm].} \quad (19)$$

The calculations used the gas layer temperature of 1000 K [38], gas plasma expansion rate was equal to 0.19 cm/ μ s and thickness of the cathode gas layer within 80 ns will be 0.015 cm. The average electron energy in the bulk of the cathode gas layer was calculated at the expansion rate of explosive-emission plasma equal to $v_{expl} = 2 \text{ cm}/\mu\text{s}$:

$$E(t) = \frac{e \cdot U(t) \cdot v_{gas2} \cdot t}{2(d_{AC} - v_{expl} \cdot t)}, \text{ [eV].} \quad (20)$$

The average electron energy in the cathode gas layer in case of the AC-gap of 1.2 cm does not exceed 2 keV at an accelerating voltage of 300–350 kV (Fig. 5).

On the leading edge of the accelerating voltage pulse, all molecules are desorbed from the cathode surface and form an expanding gas layer. When the initial surface density of adsorbed molecules is 10^{16} cm^{-2} , the average

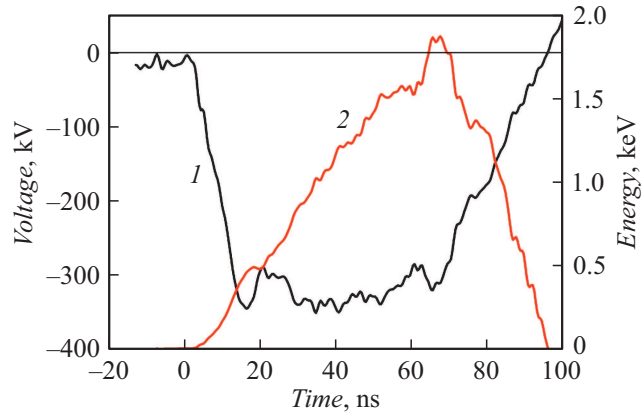


Figure 5. Oscilloscope trace of accelerating voltage (1) and change in average electron energy in the cathode gas layer during beam generation (2). Graphite cathode.

atom concentration in the cathode gas layer by the pulse end will be $\approx 7 \cdot 10^{17} \text{ cm}^{-3}$, concentration of residual gas molecules in the AC-gap being $\approx 10^{12} \text{ cm}^{-3}$. Therefore, shock ionization of molecules takes place mainly near the cathode in a desorbed gas layer of thickness d_{cath} .

As electron energy increases, LLE decrease (Fig. 3), therefore, LLE vary insignificantly during beam generation in the cathode gas layer (calculation according to the average electron energy), the average value is $45 \text{ keV/cm} \pm 4.5\%$. LLE in depth of the cathode gas layer also vary insignificantly, at the pulse end they are $45 \text{ keV/cm} \pm 4.7\%$. Therefore, a change in LLE magnitude within the cathode gas layer and during beam generation can be neglected, then in relation (18) we have $d_{AC} \approx d_{cath}$ and $n_{gas2} \cdot d_{cath} = n_{s0}$:

$$\begin{aligned} N_{sum2}(t) &= \frac{n_{gas2}(t) \cdot d_{cath}}{n_0 \cdot e \cdot E_{sum}} \frac{dE}{dx} \int_0^{\tau} I_e(t) dt \\ &= \frac{n_{s0}}{n_0 \cdot e \cdot E_{sum}} \frac{dE}{dx} \int_0^{\tau} I_e(t) dt, \text{ [ions].} \end{aligned}$$

The average (across the cathode area) concentration of cathode gas plasma is equal to

$$n_{cath1} = \frac{n_{s0}}{n_0 \cdot v_{gas2} \cdot S_{cath} \cdot t \cdot e \cdot E_{sum}} \frac{dE}{dx} \int_0^{\tau} I_e(t) dt, \text{ [cm}^{-3}\text]. \quad (21)$$

The calculation results using relation (21) are shown in Fig. 6.

3.2. Calculation according to ionization cross-section

Thickness of the cathode gas layer does not exceed 0.015 cm and energy of the electrons that form cathode gas

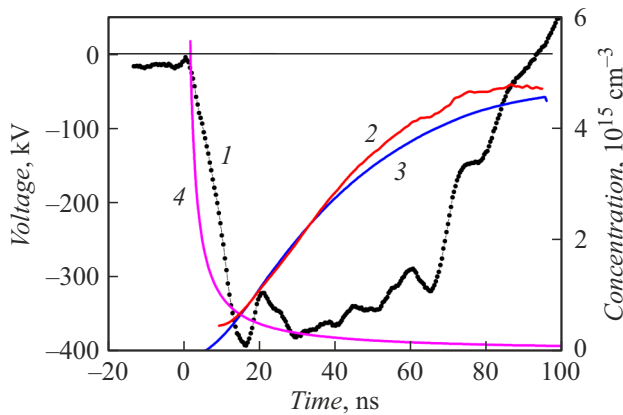


Figure 6. Oscilloscope trace of accelerating voltage (1) and change in cathode gas plasma concentration. Calculation according to LLE (2) and according to ionization cross-section (3). Curve 4 shows a change in concentration of explosive-emission plasma.

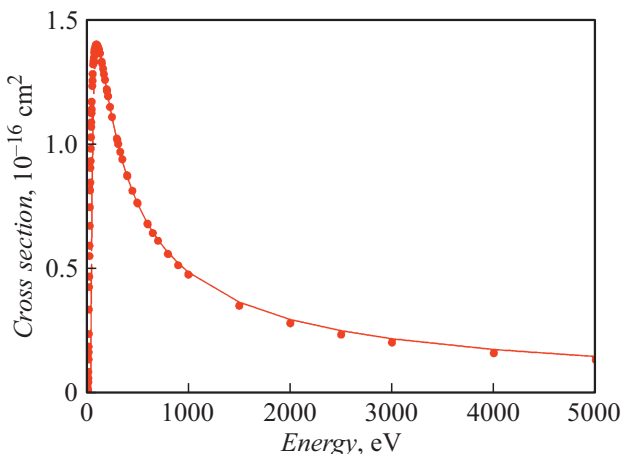


Figure 7. Dependence of cross-section of nitrogen atom shock ionization on electron energy [39].

plasma does not exceed 2 keV (Fig. 5). Concentration of cathode gas plasma can therefore be calculated according to ionization cross-section. Ionization rate for desorbed molecules is equal to

$$\frac{dn_{cath2}}{dt} = \sigma_i(t) \cdot n_{gas2}(t) \cdot \phi_e(t), \quad [\text{cm}^{-3} \cdot \text{s}^{-1}], \quad (22)$$

where σ_i is ionization cross-section, $[\text{cm}^2]$, ϕ_e is electron flux density, $[(\text{cm}^2 \cdot \text{s})^{-1}]$.

Shock ionization cross-section for nitrogen atoms as per the NIST data [39] is shown in Fig. 7.

With an electron energy of 40 eV to 5 keV, dependence of shock ionization cross-section for nitrogen atoms on electron energy was approximated by equation (Fig. 7, the line):

$$\sigma_i = 150 \cdot 10^{-16} \frac{\ln(0.025 \cdot E)}{E}, \quad [\text{cm}^2]$$

with energy in eV.

Explosive emission of electrons leads to complete desorption of molecules on the cathode working surface, and the average concentration of atoms in the cathode gas layer is equal to:

$$n_{gas2} = \frac{n_{s0}}{v_{gas2} \cdot t}, \quad [\text{cm}^{-3}]. \quad (23)$$

A change in concentration of cathode gas plasma during electric beam generation is equal to

$$n_{cath2} = \frac{0.66n_{s0}}{v_{gas2} \cdot S_{cath} \cdot e} \int_0^t \frac{\sigma_i(t) \cdot I_e(t)}{t} dt, \quad [\text{cm}^{-3}]. \quad (24)$$

The concentration of cathode gas plasma was calculated according to ionization cross-section taking into account the electron energy consumed for dissociation of nitrogen molecules, equal to 9.7 eV at the ionization energy of 14.5 eV (coefficient 0.66). The calculation results using relation (24) are shown in Fig. 6.

A decrease in electron energy during atom ionization in the cathode gas layer significantly increases ionization efficiency (Fig. 7). Average concentration of cathode gas plasma by the pulse end (on the external boundary of explosive-emission plasma) rises to $\approx 5 \cdot 10^{15} \text{ cm}^{-3}$, while thickness of the cathode gas plasma region is 0.015 cm. The average concentration of atoms in the gas layer on the external boundary of explosive-emission plasma by the pulse end is $\approx 7 \cdot 10^{17} \text{ cm}^{-3}$. Ionization degree of cathode gas plasma is equal to $\approx 10^{-2}$, which is considerably higher than the ionization degree of anode plasma.

4. Calculation of explosive-emission plasma concentration

Cathode plasma in a diode with an explosive-emission cathode is generated in case of explosive emission of electrons on the pulse leading edge. Two modes can be distinguished in plasma formation: the mode of discrete emission surface and the mode of limitation by bulk charge [2]. After application of voltage to the diode and till formation of a continuous plasma surface on the cathode (the mode of a discrete emission surface), the diode current is limited by cathode emissivity, since explosive-emission plasma on the cathode working surface originates in the form of separate emissive centers [2]. After formation of the first emissive centers, formation of other centers is suppressed due to equalization of electric field intensity (the shielding effect) [10]. Explosive emission stops after the formation of a continuous plasma layer on the cathode (concentration more than 10^{14} cm^{-3}), explosive emission stops since the plasma layer thickness considerably exceeds the micropoint height and there is no local enhancement of the electric field. Generation of new emissive centers as a result of ion current from anode plasma on the cathode surface [2,12,38] is possible only till formation of a continuous plasma layer on the cathode. Charging of dielectric inclusions and films on the cathode by an ion flow

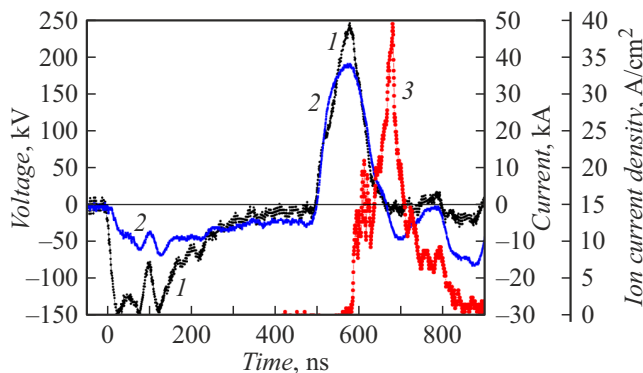


Figure 8. Oscilloscope traces of accelerating voltage (1), total current in the diode (2) and density of ion current generated by a strip ion diode (3).

from the plasma and their subsequent breakdown [38,40] are also possible only in the mode of a discrete emission surface. Therefore, electron current in the AC-gap of a vacuum diode with an explosive-emission cathode can be limited by electron concentration in cathode plasma.

The concentration of explosive-emission plasma was studied on the TEMP-4M accelerator with ion beam generation by a flat strip diode with an explosive-emission cathode in the two-pulse mode at self-magnetic insulation of electrons [41] (Fig. 8).

Ion current density was measured using a collimated Faraday cup located at the distance of 17 cm from the diode. Ion fluence ion at the ion charge density of $3.4 \cdot 10^{-6} \text{ C/cm}^2$ (integral of ion current density (Fig. 8)) is $\sim 2 \cdot 10^{13} \text{ cm}^{-2}$. A continuous layer of explosive-emission plasma forms from the plasma of separate emissive centers that originate on the pulse leading edge. Subsequently, number of ions in cathode plasma does not increase but only decreases due to emission and acceleration in the AC-gap. Then the change in explosive-emission plasma concentration during electron beam generation exclusive of electron emission is equal to

$$n_i^{\min}(t) = \frac{2 \cdot 10^{13}}{v_{\text{expl}} \cdot t}, [\text{cm}^{-3}]. \quad (25)$$

The results of the calculations using relation (25) with $v_{\text{expl}} = 2 \text{ cm}/\mu\text{s}$ are shown in Fig. 6. Explosive-emission plasma concentration after 50 ns is $2 \cdot 10^{14} \text{ cm}^{-3}$, which approaches the data presented in other papers [12,14,15].

5. Analysis of cathode plasma impact on electron beam generation

The performed studies have demonstrated that efficiency of electron beam generation in a vacuum diode with an explosive-emission cathode depends on cathode material. The use of a cathode with a developed surface (a cathode with carbon fiber coating, multipoint copper and tungsten cathodes) makes it possible to increase the total electron beam current (as compared to the calculated value as

per CL) without changing the cathode diameter and AC-gap (Fig. 2).

Electron current in a vacuum diode is limited by cathode plasma emissivity, saturation current density is equal to chaotic thermal current of cathode plasma electrons [38]:

$$\begin{aligned} j_{e0} &= en_k \sqrt{\frac{kT_e}{2\pi \cdot m_e}} = en_k \sqrt{\frac{E}{3\pi \cdot m_e}} \\ &= 0.48 \cdot 10^{-11} \cdot n_k, [\text{A}/\text{cm}^2] \end{aligned}$$

when electron energy in cathode plasma is in eV and plasma concentration is in cm^{-3} .

Then the maximum current is equal to

$$I_{e \max} = S_k \cdot j_{e0} = 14 \cdot 10^{-11} \cdot n_k, [\text{A}].$$

The maximum current for explosive-emission plasma exceeds the experimental values throughout the beam generation time (Fig. 9).

However, a high cathode plasma concentration is a required but not a sufficient condition for efficient generation of an electron beam. The total electron charge in cathode plasma must be considerably higher than the total electron beam charge during the entire pulse. Fig. 10 gives the results of the calculation of a change in total cathode plasma charge during electron beam generation. The calculation did not include electron losses for electron beam formation:

$$Q_e = S \cdot n_{\text{cath}} \cdot v_{\text{cath}} \cdot t \cdot e, [\text{C}]. \quad (26)$$

The charge of an explosive-emission plasma layer is considerably less than the electron beam charge and the main electron source is not explosive-emission plasma, but cathode gas plasma. Electron current is limited by cathode plasma concentration, since it is less than the calculated value (Fig. 2, a).

The use of carbon fiber on the cathode working surface has made it possible to increase of the total electron beam charge in 1.6 times (Fig. 2, b). Fig. 10, b gives the results of

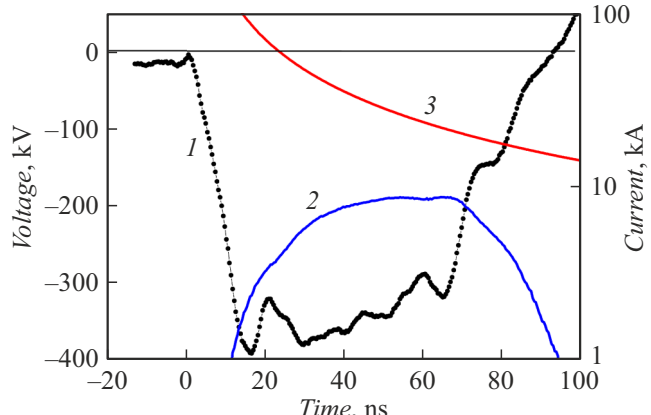


Figure 9. Oscilloscope trace of accelerating voltage (1), change in the modulus of total current in the diode (2) and the maximum current for explosive-emission plasma (3). Graphite cathode.

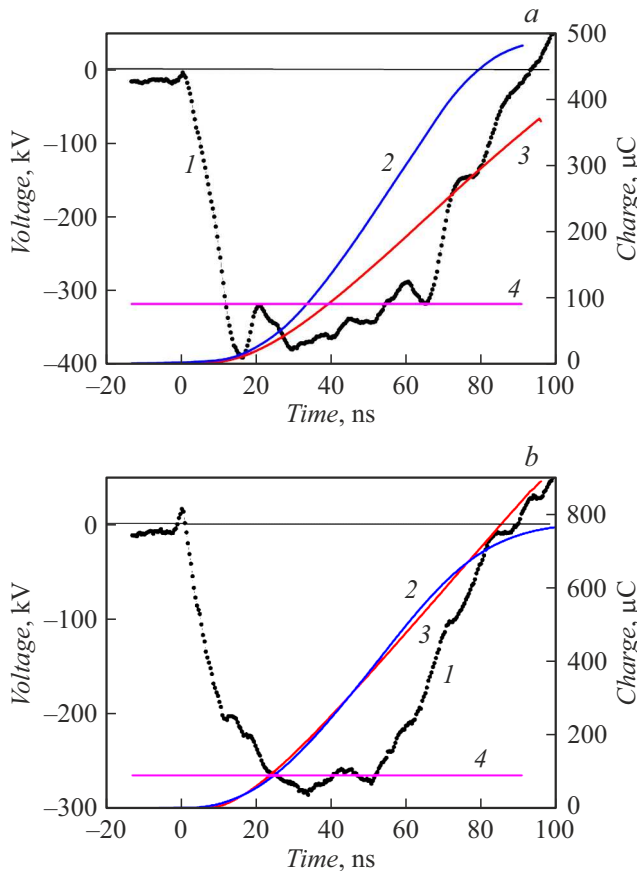


Figure 10. Oscilloscope trace of accelerating voltage (1), change in electron beam charge (2), total charge of cathode plasma (3) and charge of the explosive-emission plasma layer (4). Cathode made of graphite (a) and with carbon fiber coating (b).

the calculation of a change in total cathode plasma charge during electron beam generation by a diode with a carbon fiber cathode, cathode area is 25% larger. An increase of the area of sorption on the carbon fiber surface increased the concentration of desorbed molecules in the cathode gas layer and the concentration of cathode gas plasma. The total charge of explosive-emission plasma is limited by the number of centers of electron explosive emission on the cathode surface due to the shielding effect and will be identical for graphite and carbon fiber cathodes 6 cm in diameter. In the calculations (the integral of relation 25) it was $90 \mu\text{C}$.

Conclusion

The low efficiency of electron-stimulated desorption of molecules from the anode working surface (less than one molecule per electron) and insignificant linear losses of electron energy (less than 20 eV/cm) in the anode gas layer ensure a low anode plasma concentration not exceeding 10^{10} cm^{-3} , anode plasma ionization degree less than 10^{-3} . Pressure in the anode gas layer insignificantly exceeds the

residual gas pressure in the AC-gap during diode operation in technical vacuum. The anode plasma expansion rate is $\sim 0.17 \text{ cm}/\mu\text{s}$ and the plasma layer thickness does not exceed 1% of the AC-gap, the pulse duration being 100 ns. Therefore, anode plasma does not make a considerable contribution to the operation of a vacuum diode with a passive cathode in case of pulse durations shorter than $0.1 \mu\text{s}$.

A considerably higher concentration is observed in cathode gas plasma that originates during molecule desorption from the cathode surface, their dissociation and shock ionization of atoms. Full desorption of molecules from the cathode working surface and high efficiency of atom ionization in the cathode gas layer ensure a high plasma concentration $\sim 10^{16} \text{ cm}^{-3}$ and a high ionization degree that reaches 10^{-2} .

The charge of an explosive-emission plasma layer is considerably less than the electron beam charge and the main electron source is not explosive-emission plasma, but cathode gas plasma. For this reason, electron current is limited by cathode plasma concentration. The use of a cathode with a developed surface (a cathode with carbon fiber coating, multipoint copper and tungsten cathodes) makes it possible to increase the total electron beam charge in more than 1.5 times without changing the cathode diameter and the AC-gap.

Funding

The study was funded by RFBR within the framework of scientific project № 19-38-90001.

Conflict of interest

The authors declare that they have no conflict of interest.

References

- [1] S.P. Bugayev, Yu.E. Krendel, P.M. Shchanin. *Elektronnye puchki bolshogo secheniya* (Energoatomizdat, M., 1984) (in Russian)
- [2] G.A. Mesyats. *Impulsnaya energetika i elektronika* (Nauka, M., 2004) (in Russian)
- [3] S.Yu. Sokovnin. *Nanosekundnye uskoriteli elektronov dlya radiatsionnykh tekhnologiy* (Izd-vo Uralskogo GAU, Yekaterinburg, 2017) (in Russian)
- [4] Yu.A. Kotov, S.Yu. Sokovnin, M.E. Balezin. ZhTF, **73** (4), 124 (2003) (in Russian).
- [5] Ya.E. Krasik, A. Dunaevsky, J.Z. Gleizer, J. Felsteiner, Yu.A. Kotov, S.Yu. Sokovnin, M.E. Balezin. J. Appl. Phys., **91**, 9385 (2002). DOI: 10.1063/1.1476964
- [6] E.N. Abdullin, G.P. Bazhenov. ZhTF, **51** (9), 1969 (1981) (in Russian).
- [7] I. Langmuir. Phys. Rev., **2**, 45, (1913).
- [8] R.K. Parker, R.E. Anderson, C.V. Duncan. J. Appl. Phys., **45** (6), 2463 (1974).
- [9] A.I. Pushkarev, R.V. Sazonov. *Pribory i tekhnika eksperimenta*, 6, 103 (2008) (in Russian).
- [10] S.Ya. Belomytsev, S.D. Korovin, G.A. Mesyats. Pisma v ZhTF, **6** (18), 1089 (1980) (in Russian).

- [11] I.V. Pegel. *Nestatsionarnye protsessy generatsii silnotochnykh elektronnykh puchkov i moshchnykh impulsov elektromagnitnogo izlucheniya*. Thesis for the degree of Doctor of Physical and Mathematical Sciences (Tomsk, 2006), 213 p. (in Russian).
- [12] G.A. Mesyats, D.I. Proskurovsky. *Impulsnny elektrichesky razryad v vakuumme* (Nauka, Novosibirsk, 1984) (in Russian)
- [13] Li Limin, L. Chang, J. Liu, G. Chen, J. Wen. *Laser and Particle Beams*, **30** (4), 541 (2012).
- [14] D. Yarmolich, V. Vekselman, V.Tz. Gurovich, J.Z. Gleizer, J. Felsteiner, Ya.E. Krasik. *Phys. Plasmas*, **15**, 123507 (2008).
- [15] D.I. Proskurovsky. *Plazmennaya elektronika* (Izd-vo TPU, Tomsk, 2010) (in Russian)
- [16] A.I. Pushkarev, Yu.N. Novoselov, R.V. Sazonov. *Pribory i tekhnika eksperimenta*, **5**, 117 (2007) (in Russian).
- [17] Yu.I. Isakova, A.I. Pushkarev, G.E. Kholodnaya. *Pribory i tekhnika eksperimenta*, **2**, 39 (2011) (in Russian).
- [18] A.I. Pushkarev. *ZhTF*, **78** (3), 78 (2008) (in Russian).
- [19] V.N. Ageyev, O.P. Burmistrova, Yu.L. Kuznetsov. *UFN*, **158** (3), 389 (1989) (in Russian).
- [20] C.E. Young, J.E. Whitten, M.J. Pellin, D.M. Gruen, P.L. Jones. *Proceedings of the Fourth International Workshop Desorption Induced by Electronic Transitions DIET IV*, (1989), p. 187.
- [21] P. Feulner. *Proceedings of the Second International Workshop Desorption Induced by Electronic Transitions. DIET II*, (1984), p. 142.
- [22] Z.W. Gortel, H.J. Kreuzer, P. Feulner, D. Menzel. *Proceedings of the Third International Workshop Desorption Induced by Electronic Transitions. DIET III*. (1987), p. 173.
- [23] Electronic source. Available at: https://physics.nist.gov/PhysRefData/Ionization/atom_index.html
- [24] P. Sigmund. *Particle Penetration and Radiation Effects. Volume 2: Penetration of Atomic and Molecular Ions* (Springer International Publishing, 2014)
- [25] M. Berger, J. Coursey, M. Zucker, Chang J. NIST Standard Reference Database, 124 (2017).
<https://physics.nist.gov/PhysRefData/Star/Text/ESTAR.html>
- [26] T.E. Madey, R. Stockbauer. *Experimental methods in electron and photon-stimulated desorption*. In Methods of Experimental Physics: V. 22. Ed. by R.L. Park, M.G. Lagally (Academic Press Inc., 1985)
- [27] V.P. Krivobokov. *Radiatsionnye i plazmennye tekhnologii: terminologichesky spravochnik* (Nauka, Novosibirsk, 2010) (in Russian)
- [28] V.N. Ageyev, Yu.A. Kuznetsov, B.V. Yakshinsky. *FTT*, **24**, 349 (1982) (in Russian).
- [29] V.N. Ageyev, O.P. Burmistrova, B.V. Yakshinsk. *Surf. Sci.*, **194**, 101 (1988).
- [30] T.E. Madey, J.T. Yates. *J. Vacuum Sci. Technol.*, **8**, 525 (1971).
- [31] D. Menzel. *Topics Appl. Phys.*, **4**, 101 (1975).
- [32] P.H. Dawson. *Surf. Sci.*, **65**, 41 (1977).
- [33] V.E. Mironov, B.A. Shestakov. Soobshcheniya obyedinenного instituta yadernykh issledovaniy. Dubna. 9-86-304, 1–7. (1986) (in Russian).
- [34] A. Fridman. *Plasma Chemistry* (Cambridge Univer. Press, NY, 2008)
- [35] P.M. Bellan. *Fundamentals of Plasma Physics* (Cambridge Univer. Press, 2006)
- [36] V.S. Vorob'ev. *Plasma Sources Sci. Technol.* **4**, 163 (1995).
- [37] L.M. Biberman, V.S. Vorobjev, L.T. Yacubov. *Adv. Phys. Sci.*, **107**, 353 (1972).
- [38] G.E. Ozur, D.I. Proskurovsky. *Istochniki nizkoenergeticheskikh silnotochnykh elektronnykh puchkov s plazmennym anodom* (Nauka, Izd-vo SO RAN, Novosibirsk, 2018) (in Russian)
- [39] Y.-K. Kim, J.-P. Desclaux. *Phys. Rev. A*, **66**, 012708 (2002). https://physics.nist.gov/cgi-bin/Ionization/ion_data.php?id=NI&ision=I&initial=&total=Y
- [40] G.A. Mesyats. *PMTF*, **5**, 138 (1980) (in Russian).
- [41] A.I. Pushkarev, Yu.I. Isakova, R.V. Sazonov, G.E. Kholodnaya. *Generatsiya puchkov zaryazhennykh chastits v diodakh so vzryvoemissionnym katodom* (Fizmatlit, M., 2013) (in Russian)